buildings

MDPI

Article

Preliminary Geospatial and In Situ Reconnaissance of the 8 September 2023 Moroccan Atlas Earthquake Damage

Beatriz González-Rodrigo [1,*], Laura Navas-Sánchez [2], Juan Gregorio Rejas-Ayuga [3,4,*], Orlando Hernández-Rubio [5] and María Belén Benito [6]

1 School of Forest Engineering and Natural Resources, Universidad Politécnica de Madrid (UPM), 28040 Madrid, Spain
2 Construcciones Arquitectónicas, Universidad Rey Juan Carlos (URJC), 28942 Madrid, Spain; laura.navas.sanchez@urjc.es
3 School of Civil Engineering, Universidad Politécnica de Madrid (UPM), 28040 Madrid, Spain
4 National Institute for Aerospace Technology (INTA), 28850 Madrid, Spain
5 Geolyder SL, 28020 Madrid, Spain; orlando.hernandez@geolyder.com
6 School of Surveying, Geodesy and Cartography Engineering, Universidad Politécnica de Madrid (UPM), 28031 Madrid, Spain; mariabelen.benito@upm.es
* Correspondence: beatriz.gonzalez.rodrigo@upm.es (B.G.-R.); juangregorio.rejas@upm.es (J.G.R.-A.)

Abstract: This research investigates the post-earthquake performances of structures in four rural villages in the Moroccan Atlas, emphasizing common construction system characteristics and design flaws that render buildings susceptible to seismic events. Village selection was based on a prior multispectral satellite-image study, proving effective for planning high-impact, post-earthquake field campaigns. The significance of this research resides in on-site data collection, facilitating the physical assessment of earthquake-induced damage and identification of inherent vulnerabilities in construction systems. The constructions in the study area exhibited structural design deficiencies, inadequate construction techniques, and urban modifiers, leading to damage extensively documented in the literature, as well as less-documented unique damage. Predominant seismic-design shortcomings in the study area included subpar material quality, insufficient earthquake-resistant design, and unskilled labor. In situ data were complemented by a global geospatial approach using differential synthetic aperture radar interferometry with Copernicus Sentinel 1 data. Once calibrated the proposed methodology with field data, the analysis of remote sensing processing results, allow assessing the damages in other earthquake-affected areas, including those not visited in the field but also impacted by the seismic event.

Keywords: seismic vulnerability; urban modifiers; seismic structural design; geospatial analysis; DInSAR

Citation: González-Rodrigo, B.; Navas-Sánchez, L.; Rejas-Ayuga, J.G.; Hernández-Rubio, O.; Benito, M.B. Preliminary Geospatial and In Situ Reconnaissance of the 8 September 2023 Moroccan Atlas Earthquake Damage. *Buildings* **2024**, *14*, 693. https://doi.org/10.3390/buildings14030693

Academic Editor: Giuseppina Uva

Received: 19 January 2024
Revised: 19 February 2024
Accepted: 21 February 2024
Published: 5 March 2024

1. Introduction

On the night of 8 September 2023, an earthquake measuring magnitude Mw 6.8 struck the High Atlas Mountain range in Morocco, reaching a depth of 26 km below the surface. This seismic event was followed by multiple aftershocks, including a Mw 4.9 aftershock just 19 min after the main tremor. The impact was severe, resulting in close to 3000 casualties and extensive damage to tens of thousands of buildings. Notably, this earthquake stands as the strongest Morocco has experienced in the last century [1], exceeding the expected Design Basis Earthquake (DBE) level indicated in seismic hazard maps, which projected a DBE of up to 0.18 g in the affected area [2]. The discrepancy in seismic intensity may be attributed to the limited historical seismic data available for this region. Surprisingly, there are no recorded ground motions for this event available, complicating efforts to analyze and understand this disaster. As a result of intense shaking and inadequate construction practices employing fragile systems such as unreinforced masonry and earth structures, destruction in rural regions, particularly mountain villages, was severe.

This article examines the post-earthquake behavior of structures in four rural villages nestled within the Moroccan High Atlas Mountains, focusing on the distinct characteristics of commonly used construction systems and design flaws that render buildings vulnerable to such events. The significance of this research resides in the on-site data collection, enabling the physical assessment and analysis of earthquake-induced damage, as well as the identification of vulnerabilities inherent to the construction systems employed.

The multidisciplinary study carried out comprises the following aspects. Firstly, a general study of the region is conducted: Section 2 analyzes the seismotectonic context, Section 3 introduces the building typologies generally found in the affected areas and the damage sustained in these areas in previous events, and Section 4 presents the methodology employed for selecting the areas to be visited, emphasizing the potential of remote sensing techniques for planning post-earthquake field campaigns in areas with limited exposure data. Next, within the field campaign, Section 5 contributes a detailed examination of the data collected in situ on the vulnerability of the construction systems found in the areas visited, the seismic behavior they presented, and the most typical or significant damage suffered, along with the associated causes. Finally, Section 6 provides the conclusions as well as a series of proposals for future lines of research resulting from the cross-functional approach employed.

2. Seismotectonic Context

The regional tectonics underlying Morocco's seismicity is framed by the boundary of the Eurasian and African plates and is governed by the convergence of both tectonic plates. This boundary is broadly defined between the Azores and west of the Gibraltar Strait, where large earthquakes have occurred, Mw > 6, with epicenters aligned along the contact of the two plates, such as the Lisbon earthquake of 1755 (Mw ≈ 8.5), and other more recent earthquakes in 1915 (Mw = 6.2), 1941 (Ms = 8.4), 1964 (Ms = 6.4), 1969 (Mw = 7.8), and 2007 (Mw = 6.1) [3]. However, to the east of the Strait of Gibraltar, seismicity is more diffuse and of lower magnitude, characteristic of collision zones between continental plates with a wide deformation band. This convergence between plates also explains the orogeny of the Betic mountain belt range in southern Spain and the Atlas Mountains in Morocco. Figure 1 shows this tectonic environment and the associated seismicity.

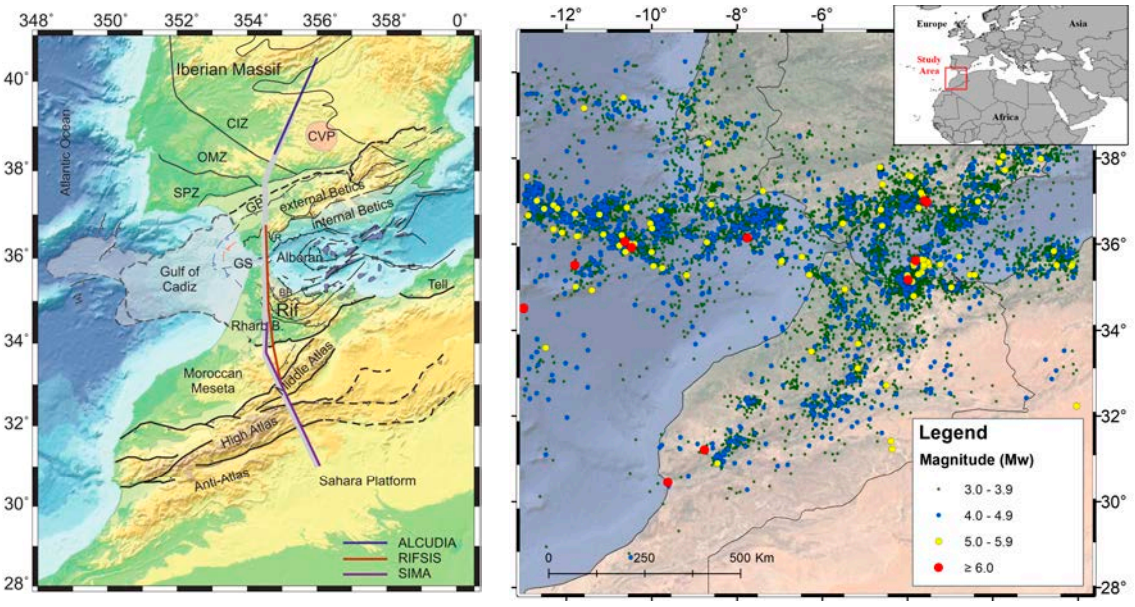

(**a**) (**b**)

Figure 1. (**a**) Tectonic framework of the South Iberian Peninsula and North Africa, a convergency region of the Eurasian and African plates [4]. (**b**) Sources of seismicity in the region (source of data: IGN).

At present, these plates converge in a northwest–southeast (NW–SE) direction with a velocity of approximately 5 mm/yr near the Strait of Gibraltar and a velocity of about 8 mm/year along the length of Tunisia. The convergence between the two tectonic plates is mainly accommodated in the Betic ridge in Spain and the Atlas mountains in Morocco.

The geological structure and evolution of Morocco are complex and consist of alternating periods of quiescence and tectonic deformations that have structured the different zones. The geological structure of Morocco includes four main domains, each characterized by a specific orogeny: (1) the Precambrian domain corresponding to the Anti-Atlas and the northern part of the West African Craton; (2) the Caledonian–Hercynian domain, which corresponds to the Moroccan Plateau; (3) the Atlas domain, which includes the High and Middle Atlas intracontinental belts; (4) and, finally, the Rif domain, corresponding to the Rif Alpine belt and its foreland basins. These domains are separated from each other by a system of faults, the activity of which has been important throughout the geological history of the region [3].

In this tectonic complex, the region of Morocco has experienced several significant earthquakes throughout its recent history, with the highest magnitudes ranging from Mw 6 to 6.3. Analysis of the macroseismic and instrumental data shows that the seismicity is relatively moderate and is concentrated in the Rif domain, mainly in the Al Hoceima region, in the Middle and High Atlas and in the Western Rif where a significant NW-SE seismic alignment is observed, starting roughly in the vicinity of Fez and passing between Larache and Asilah through Ouezzane. Analyzing the distribution of earthquake epicenters in the instrumental period, three seismic domains can be differentiated [3].

(1) The Atlas domain, where the seismic activity is mainly located in the Middle Atlas and the Central High Atlas. This seismicity is due in large part to the presence of a complex network of active faults. The South Atlas Fault, which starts from Agadir and passes close to Figuig, is marked by violent earthquakes such as that of Agadir (1960, Mw = 5.9). Although the latter was an earthquake of less than magnitude 6, it was the most devastating to occur in Morocco, striking the coastal region near Agadir and claiming approximately 15,000 lives.
(2) Betic–Rif domain: the area between south-eastern Spain to the north and the Rif belt to the south is an intense location where the seismic activity highlights the convergence and collision of the African and Eurasia tectonic plates. This convergence is marked by severe earthquakes in southeastern Spain, in the Alboran Sea and northern Morocco, such as the recent earthquakes in Al Hoceima of 2004 (Mw 6.3) and 2016 (Mw 6.2).
(3) The Atlantic domain: where the boundary between the two plates, represented by the Azores Gibraltar Sicily seismic line, can be clearly distinguished. This is punctuated by earthquakes of magnitude 6 or greater. Moreover, these oceanic earthquakes, particularly those located SW of Cape St Vincent, affect the Iberian Peninsula and Morocco, as was the case in the earthquakes of 1755 (M $\approx$ 8.5) and 1969 (Ms = 7.3), which largely affected northern Morocco.

The recent earthquake that occurred on 8 September 2023 is part of the Atlas tectonic domain. Compared to other seismically active parts of different structural domains of Morocco, the Atlas domain is considered to be a significant seismicity area after the Rif domain, since this latter is close to a high-tension continental collision zone [5]. However, sparse and diffuse seismic activity are still observed in the Atlas chain region over the three distinct Atlas blocks (Middle, High and Anti-Atlas) (Figure 2). To the south, in the Sahara region, no seismic activity is generally observed and the seismicity decreases along the eastern High Atlas [3]. According to the worldwide teleseismic catalogues, this Atlas seismicity corresponds mostly to Mw < 5 events, and only two Mw > 5.5 events were recorded over the last 40 years on the eastern Anti-Atlas zone. Considering a larger time frame, the largest earthquake ever recorded within the Atlas Region was the destructive Agadir earthquake on 29 February 1960. The Atlas region is thus characterized by moderate seismic activity, similar to most seismic areas of Western Europe [6].

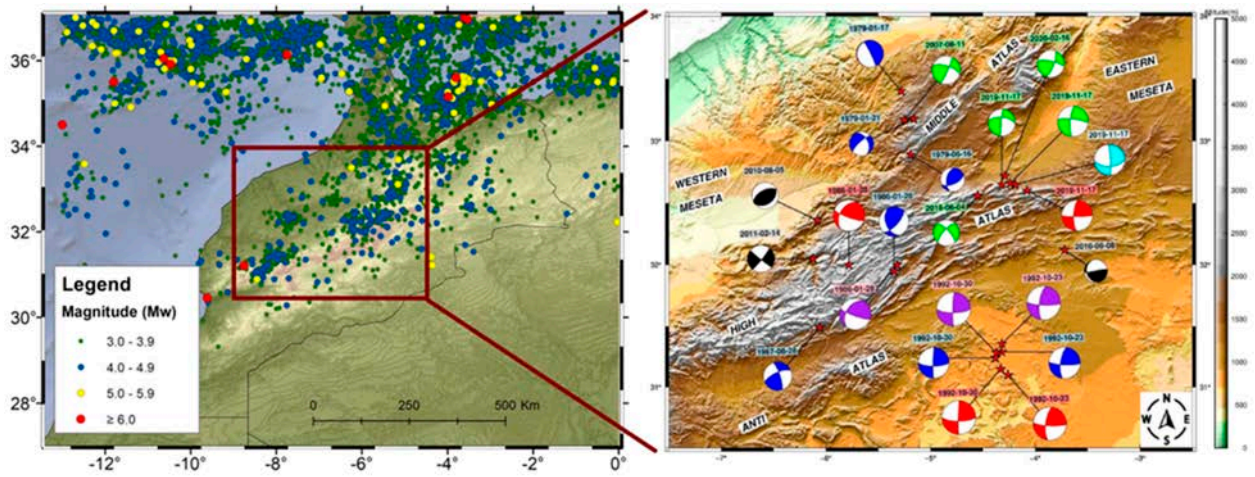

(**a**) (**b**)

Figure 2. (**a**) Distribution of epicenters in Morocco and surrounding area for earthquakes with Mw > 3 (source of data IGN). (**b**) Focal mechanism for the earthquakes in the Atlas domain in the region within the rectangle in Figure 2a [6].

Seismic events in the Atlas are generally caused by local active tectonic deformations and by the major faults related to the regional geodynamic process of the oblique NW–SE convergence between the Nubian and Eurasian plates at a rate of ~5 mm/year [5]. Consequently, the regional distribution of the Atlas earthquake epicenters appears to emphasize a rugged NE–SW trend, which is sub-parallel to the Middle Atlas chain, but oblique to the WSW–ESE orientation of the High Atlas [6]. Many east–west and northeast–southwest strike-slip and thrust faults are found in the High Atlas. Figure 2 shows the seismicity of the three domains affecting Morocco and the focal mechanism in faults of the Atlas domain.

Local Tectonic and Characteristics of the 8 September 2023 Event

More specifically, the epicenter of the 8 September earthquake was located in the western part of the High Atlas (WHA). There has not been a Mw 6.0 or larger earthquake within 500 km of the epicenter of the recent earthquake since 1900. The WHA range covers several Atlantic coastal basins and their adjacent Atlantic shelf segment. This large area evolved as a part of the Atlantic passive margin during the Triassic to Lower Cretaceous periods, with NNW–SSE compression developing from the Upper Cretaceous to the present due to convergence between Africa and Europe. This compression resulted in reverse faulting [5].

The earthquake struck at 11:11 pm local time near the town of Oukaimedene in western Morocco, and the epicenter was located in Al Haouz Province, 72 km southwest of Marrakech at a depth of 19 km [7]. The focal mechanism given by different agencies indicates oblique-thrust faulting beneath the High Atlas. A finite fault model by the United States Geological Survey (USGS) [7] indicates that rupture occurred on an east-northeast–west-southwest striking, north–northwest dipping thrust fault. Slip was mostly concentrated around the hypocenter within an elliptical slip patch measuring approximately 30 km long by 25 km wide. A maximum displacement of 1.9 m was observed. Figure 3 illustrates the location of the main shock and aftershocks, and the solutions regarding the slip and focal mechanism estimated by different agencies.

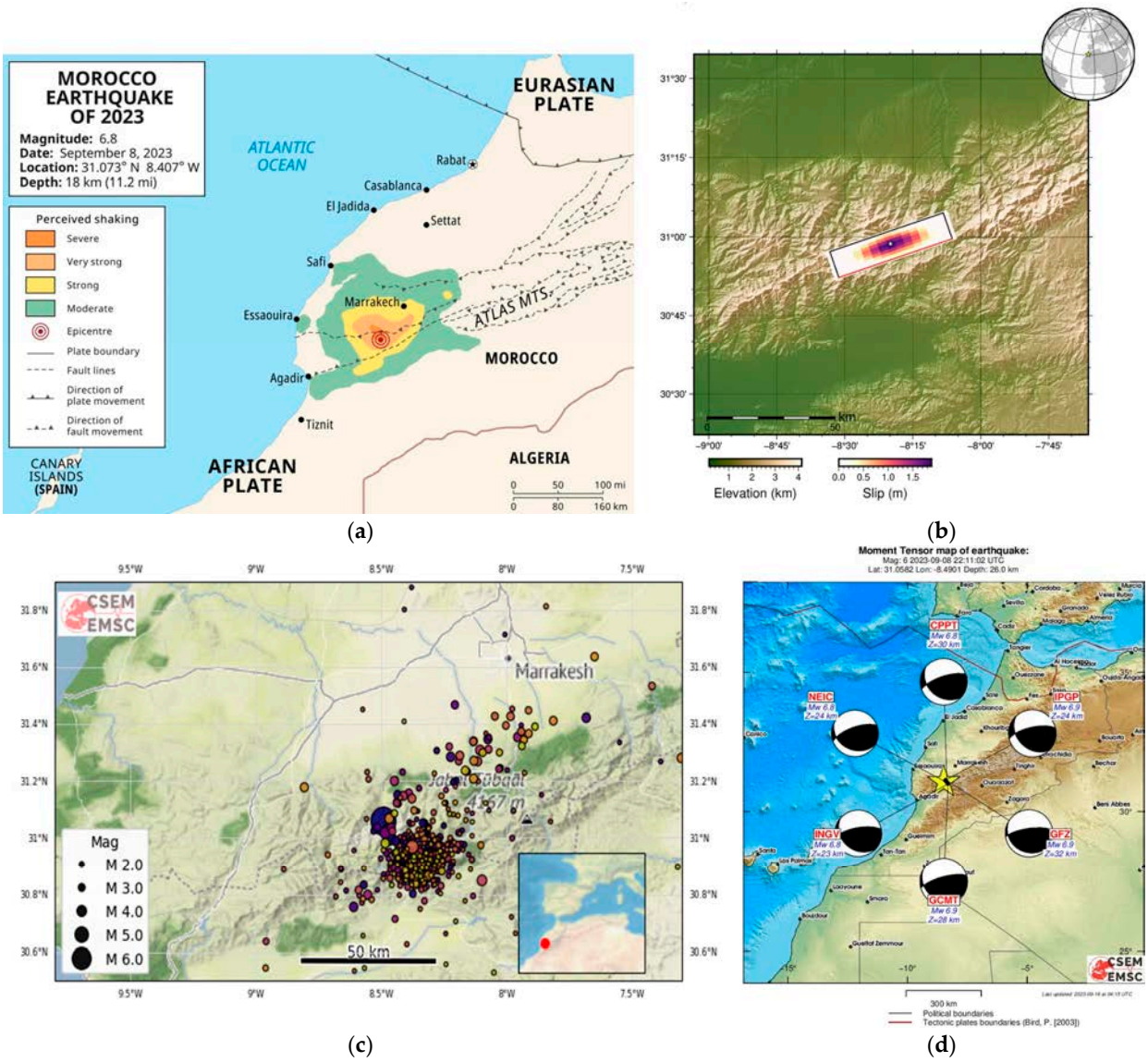

Figure 3. (**a**) Location and macroseismic area of the 8 September (2023) earthquake in the western zone of High Atlas (www.britannica.com/event/Morocco-earthquake-of-2023, accessed on 18 January 2024). (**b**) Slip model estimated by USGS [7]. (**c**) Aftershock distribution in the first ten days [8]. (**d**) Focal mechanism solutions given by different agencies for the main shock [8].

According to the data provided by USGS, the maximum intensity of VIII (IMM) was reported in the towns of Amizmiz, Azgour, Adassil and Tisguine, although the earthquake was felt in an extensive macrosismic area, including locations in the Iberian Peninsula (Figure 4).

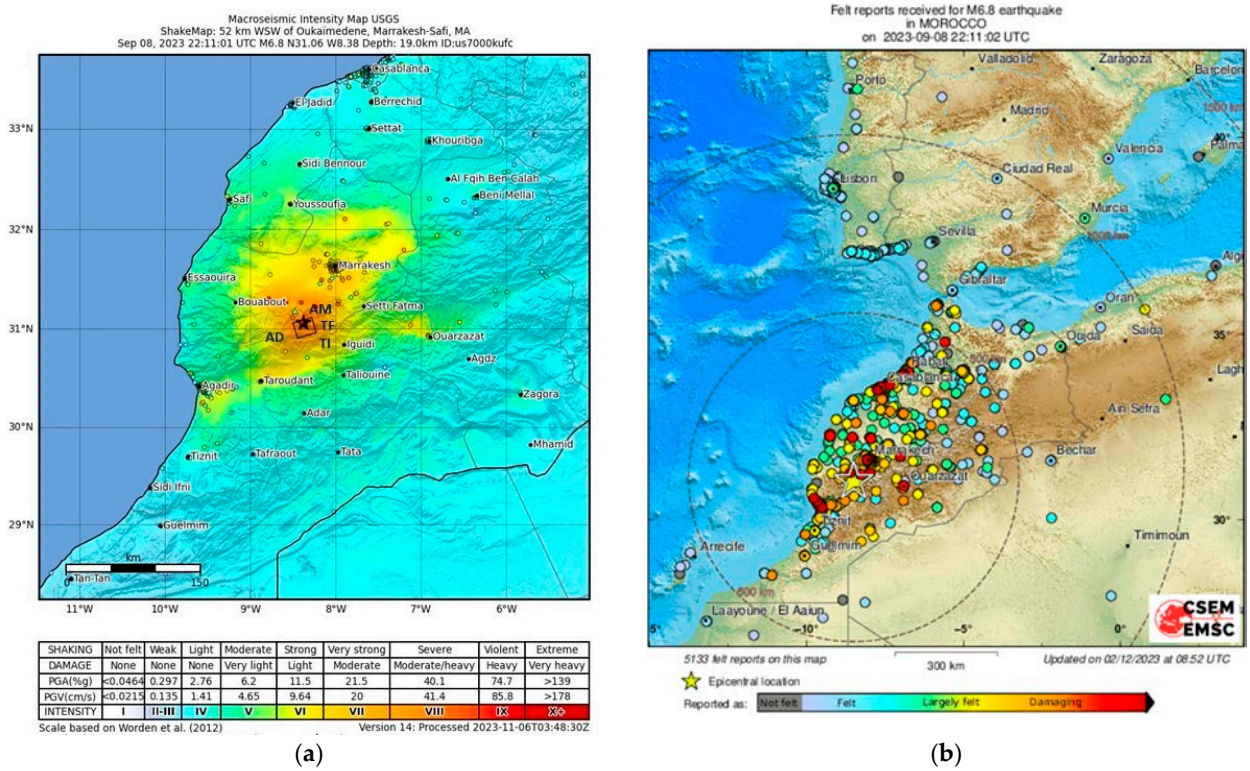

Figure 4. (**a**) Isoseismal map for the most affected area, IMM scale (USGS) (USGS), [7]. Am.: Amizmiz, Ad.: Adassil, Tf.: Tafeghaghte, Tl: Talat N'Yaqoud. (**b**) Local intensities in different populations of North Africa and South Iberian Peninsula where the main shock was felt, IMM scale (EMSC) [9].

3. Building Typology in the Affected Area

In general terms, constructions in Morocco reflect a combination of developing building regulations, diverse construction practices in urban and rural areas, and a multitude of socio-economic and cultural elements. The earthquake-affected region not only bears the scars of seismic activity but also boasts a profound heritage of vernacular architecture intimately connected to the climatic nuances and native building materials of the area. Within this region, rural areas epitomize the prevalence of vernacular construction systems—embracing techniques like rammed earth walls, limestone, or shale masonry. These techniques often support unidirectional wooden flooring or thatched roofs covered by compacted soil.

In these rural landscapes, settlements have historically emerged from the interplay between the primary village (douar) and secondary high-altitude settlements (azib), leaving a distinct imprint on both construction methods and housing designs. The earth structures consist of load-bearing walls made with rammed earth for the ground and first floor and adobe walls on the third story [10]. The prominence of rammed earth walls diminishes as the altitude of the settlements increases, yielding space to the characteristic temporary structures of azib. These structures, pivotal for accommodating substantial herds of small livestock during transhumance, predominantly feature stone masonry walls and juniper wood [11]. Occasionally, these temporary structures have transitioned into enduring dwellings. However, a noticeable transformation has marked these traditional construction systems, particularly in urban centers, where modern methodologies such as confined masonry and concrete portal systems have gained ground. Amidst these advancements, mixed systems have prevailed, characterized by the erection of a second floor using a distinct system atop a foundation of vernacular rammed earth walls or stone masonry.

There has been an evolution of structural typologies within construction regulations in response to seismic concerns. Initiatives such as the *Béton Armé aux Etats Limites* (BAEL) and PS 92 (French Seismic Code) introduced seismic protective measures for buildings

in Morocco during the early 1990s [2]. Subsequently, the enforcement of *Le Règlement De Construction Parasismique* (RCP 2000) [12] in the early 2000s marked a significant step. The initial iteration of RPS 2000 categorized different construction typologies, establishing distinct 'construction classes.' The most recent update in 2011 (RCP 2000 version 2011) [13] sets specific maximum ground acceleration (PGA) values ranging from 0.04 to 0.18 g for five seismic zones.

Vulnerability of Construction Systems Analysed in the Moroccan Atlas

Rammed-earth and stone masonry structures have low structural integrity and exhibit rapid degradation in strength due to ageing and weathering. These earthen walls require a considerable thickness to resist their own weight and the transmission of vertical load, thereby increasing the inertial forces in the event of seismic loading. In the case of earth structures, due to the low compressive strength and almost zero tensile strength, it is common to observe the presence of vertical cracks throughout the height of the walls [14]. The seismic performance of stone masonry is known to be generally poor with respect to other structural typologies [15,16]. However, significant differences can be observed for different designs, structural details and mechanical properties of masonry [17]. The post-seismic analysis reveals a clear link between construction quality and the level of damage incurred [18]. Seismic damage to existing stone masonry buildings is commonly determined by specific local failure patterns, typically consisting of out-of-plane overturning of structural portions, shear damage in-plane walls with openings or crumbling of outer wythes in multi-leaf walls caused by insufficient cohesion of the stones [19]. In structures with sufficient masonry wall quality, a predominant behavior regulated by the in-plane capacity of walls can emerge and determine the overall failure mode, given that appropriate interlocking between perpendicular walls and between walls and floors effectively counteracts the initiation of localized failures. In such scenarios, the stiffness of horizontal elements such as floors and roofs can notably influence the correlation of responses among various walls, consequently influencing the overall capacity of the building [17].

In the Mw 6.2 Al Hoceima earthquake of 2004, earth and masonry structures sustained significant damage, with the most common issues stemming from the cyclical inversion of deformation in two perpendicular walls meeting at a corner, resulting in brittle failure in unreinforced masonry constructions. Damage due to shear was also observed in the ground-floor walls of these stone or earthen masonry systems. Furthermore, in stone masonry structures, the poor mortar employed in traditional construction often results in a behavior approaching that of two independent walls. A commonly observed type of damage is the loss of one of the two walls [20]. These same failures in stone masonry walls have been reported in post-seismic studies carried out in different countries [15,19,21].

4. Methodology for Field Campaign Conducted in the High Atlas of Morocco

4.1. Selection of the Study Area

The field campaign was planned based on the information published about the earthquake location and its aftershocks [2], analyzing the region by means of remote sensing techniques and previous photographs of buildings, while also studying several key factors such as whether the places to be visited represent different socio-economic contexts, predominant construction systems and population densities. Four rural areas were selected as the most suitable places to visit for the purposes of this research: Amizmiz, Talat N'Yaqoud, Tafeghaghte and Adassil.

The village of Amizmiz was chosen due to its strategic geographic location, since it acts as a population center with over 10,000 inhabitants and a relatively developed urban infrastructure. This area exhibits dwellings arranged in blocks or rows, reflecting a more modern urban planning model compared to surrounding areas. Talat N'Yaqoud was included in the list due to its interconnection with economic activity and its population size, which exceeds 7000 inhabitants. Therefore, these two places provide an interesting contrast in terms of population density, modern construction systems and level of urbanization.

In contrast, Tafeghaghte, a rural village in the Atlas Mountains near Amizmiz, was selected because of its predominant stone masonry construction system, which proved highly vulnerable during seismic events. The tragic loss of over half of its small population of 160 inhabitants during the last earthquake highlights the urgent need to better understand the influence of building structure on mitigating seismic risk. The choice of Adassil, located a short distance from the epicenter and with a predominant construction system of compacted earth, was based on the need to understand how this type of construction behaves in seismic events, in addition to its geographical proximity for the purpose of direct comparisons with other study areas.

Furthermore, within these villages, a more detailed remote sensing analysis was employed, so as to identify the specific areas that could contribute more valuable information to the research. The diversity of these contexts allows for a multidimensional analysis of structural typologies, urban planning, and their relationship with seismic vulnerability in rural communities, thus providing a comprehensive framework.

4.2. Field Campaign Planning: Geospatial Images and Pre-Processing

In order to plan the specific areas to visit in the field campaign conducted between 2 and 6 November 2023, we carried out an analysis of multi-scale, micro, medium and macro-scale, and multi-temporal satellite images from before and after the earthquake (Figure 5). The images and data used correspond to the approach described in [22]. This procedure was performed with the aim of obtaining a first quantitative approximation of the impact of the earthquake on buildings and manmade structures. Hence, a set of images of the different affected areas was acquired from the various platforms, as presented in Table 1.

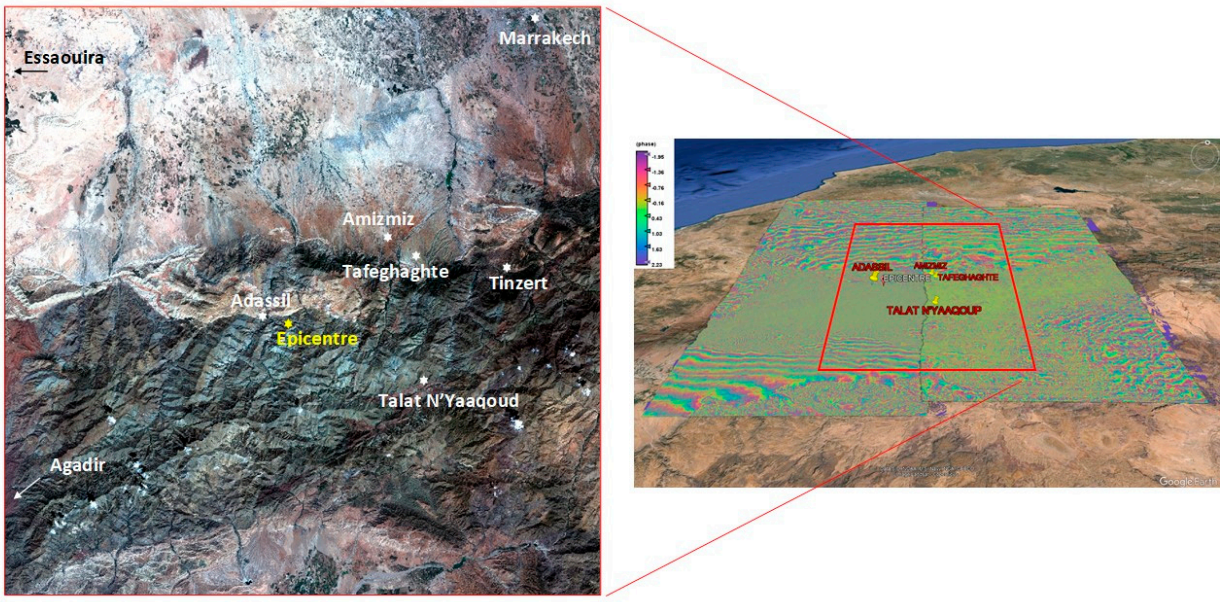

(**a**) (**b**)

Figure 5. (**a**) Copernicus Sentinel-2 image from August 2023 over the study area (**b**) Interferogram computed from Sentinel-1 radar images (3–15 September 2023) showing land deformation patterns in this period.

Table 1. Characteristics of images employed in the field campaign planning.

Zone	Coordinates (WGS34)	Epicentral Distance Orientation	Image Size Spatial Resolution	Before Date After Date	Copyright Image
Amizmiz	31°12′53.06″ N 8°14′48.87″ W	22 Km 57° N	1578 × 940 pixels 0.5 m	September 2020 October 2023	Airbus Airbus
Tafeghaghte	31°11′48.01″ N 8°13′25.74″ W	23 Km 65° N	1564 × 930 pixel 0.5 m	June 2022 September 2023	Maxar Technologies Airbus
Adassil	31°7′6.72″ N 8°29′27.02″ W	5 Km 238° N	1572 × 933 pixel 0.5 m	April 2022 October 2023	Maxar Technologies Airbus
Talat N'Yaqoud	30°59′31.28″ N 8°11′2.32″ W	27 Km 118° N	1577 × 939 pixel 0.5 m	June 2022 September 2023	Maxar Technologies Airbus

It was necessary to transform the parameters of the images to an absolute scale, both spatial and spectral, so that the extracted measurements can be linked or compared to others from the different sensors taken on different dates or related to those taken on the ground. The objective is to prepare the data set for subsequent analyses that will allow spatial correlation of the elements of seismological interest in this case (buildings, walls, surfaces, structures, remains, roads, etc.) with biophysical parameters that will be extracted in subsequent phases of the research using remote sensing and image processing techniques.

The images, with their respective copyrights, were acquired from Google Earth Pro. They have been georeferenced in the Word Geodetic System 84 geodetic reference frame and Universal Transverse Mercator coordinates for zone 29 R of this cartographic projection. New sub-scenes have been generated at 0.5 m spatial resolution, maintaining the original spectral information. Table 1 presents the matrix that describes the data used in planning the November 2023 campaign.

4.3. Exploratory Geospatial Analysis

Previous studies have demonstrated the potential of remote sensing to effectively identify the most damaged areas of a village after an earthquake (i.e., the areas with the highest percentage of severely damaged and collapsed buildings). However, identifying areas with lower levels of damage can be more difficult, and also requires field data [23].

Exploratory geospatial analysis techniques were applied to the pre-processed images in order to contrast them and perform an approximate quantitative evaluation prior to collecting information on the effects of the earthquake in situ. For this purpose, the following two techniques were employed: firstly, that of calculating both the soil index Redness Index RI [24] and vegetation Soil Adjusted Vegetation Index SAVI [25] to separate the land cover from buildings and manmade structures, and secondly, a technique termed change dynamics, based on digital image classification.

Digital image classification consists of a set of procedures that allow the pixels of an image to be automatically categorized into different types of clusters (see Figure 6, below). Damage detection in post-earthquake satellite images can be improved through field observations [26,27], for example, since these observations provide the real information needed to estimate the error in digital classification processes of optical images by calculating confusion or contingency matrices.

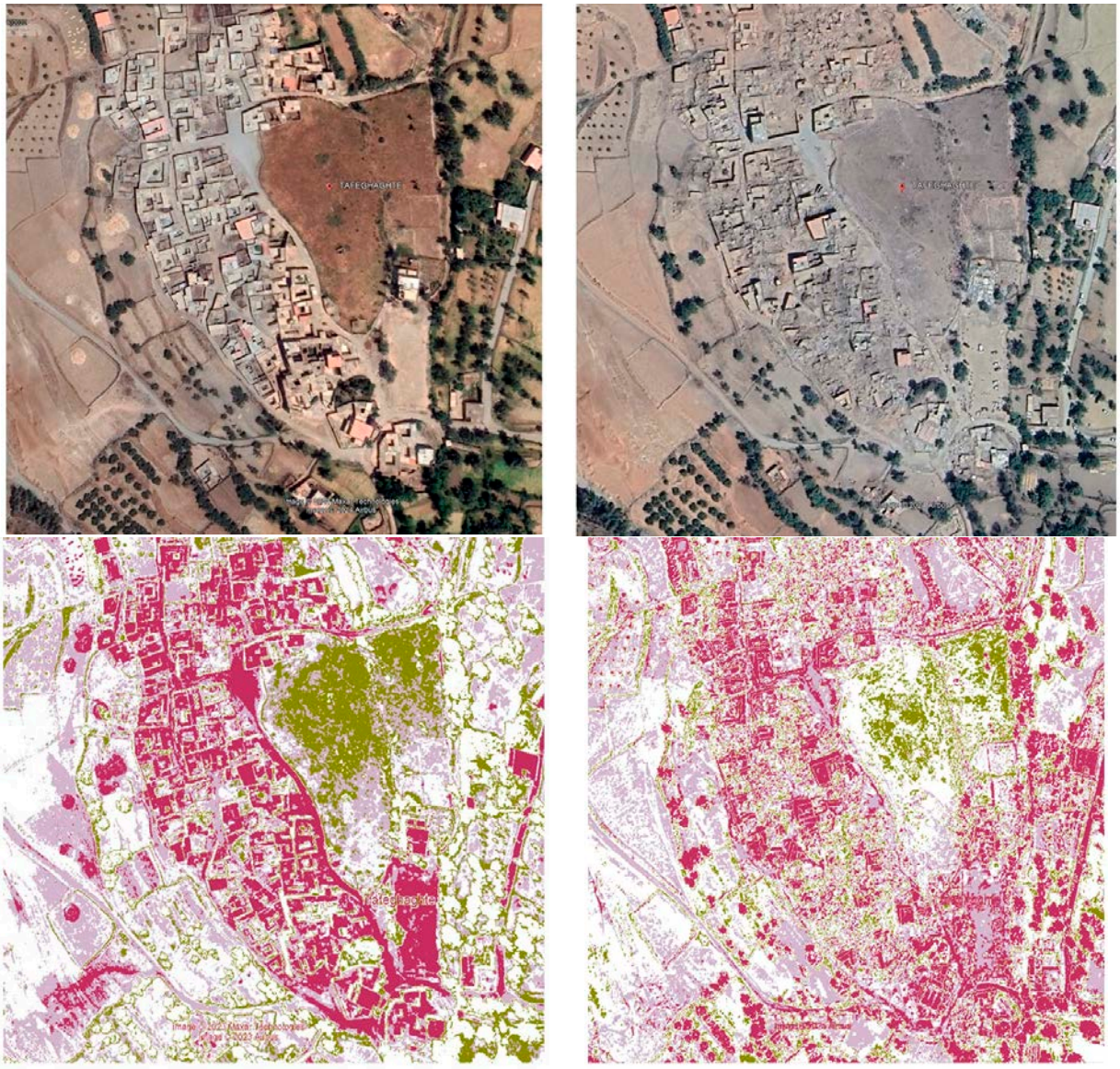

(**a**) (**b**)

Figure 6. Detail of Tafeghaghte before (06/2022) and after (10/2023) the occurrence of the earthquake of 8 September 2023, (**a**,**b**), respectively. Digital classifications of typologies using the k-means algorithm in which two classes of interest (cluster 6 and 7) for research are highlighted, covered by buildings and artificial structures such as roads and streets.

In our case, an unsupervised approach was followed, whereby the characteristic spectral information of the categories to be discriminated is incorporated, identifying a set of pixels that correspond to the same quantitatively defined category without the need for prior knowledge; that is, a 'brute-force' procedure in which the computer acts automatically. The classification process iteratively compares the rest of the image pixels with the reference values of the established categories, assigning them to that which is most similar based on some type of indicator which assesses their spectral similarity, in this case, through the k-means clustering algorithm [28].

The results were initially strongly influenced by the vegetation cover, which acts as a reflectance input error in the calculation of the new variables or clusters, so a mask extracted from the calculated vegetation indices was generated. A total of seven clusters were defined, of which the last two corresponded to the typologies of interest in the research: the sixth cluster corresponds to artificial materials such as concrete and asphalt, symbolized in gray

in the color table, and the seventh cluster to building cover, symbolized on the color table in magenta (Table 2, column "Change").

Table 2. Geospatial analysis of changes before and after the earthquake of 8 September 2023; with visited zones framed in red.

Village **% Image Change; % Structures Change**		
Image **after the Earthquake**	**Image** **before the Earthquake**	**Change**
Amizmiz −44% image change; −5% structure change		
	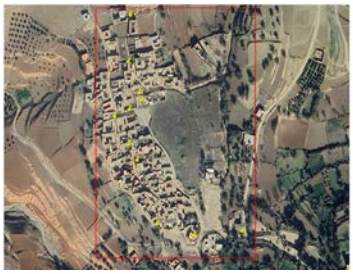	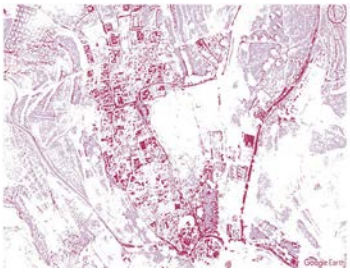
Tafeghaghte −69% image change; −27% structure change		
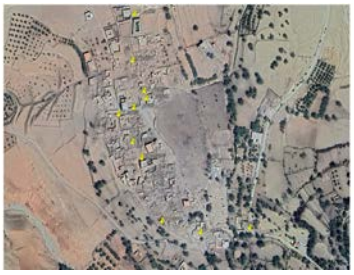	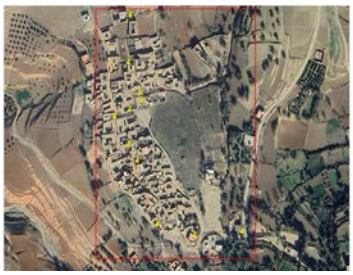	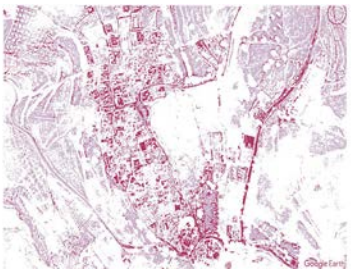
Adassil −47% image change; −21% structure change		
		
Talat N'Yaaqoud −72% image change; −35% structure change		
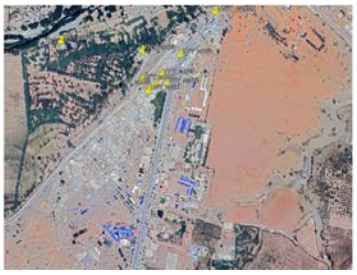		

The evaluation of the classification was performed using the matrix of errors method. The images taken in situ were used as a real value for the classes. The percentage of pixels not classified is 5% and the accuracy of the classification is about 75%, which was expected and consistent with similar studies [22] in which the k-means algorithm has been applied. A certain level of confusion, not critical to the purposes of this approach, occurred between different types of roofs and roads. Bituminous roofs are confused with concrete roads, stones and asbestos roofs are confused with asphalt roads, while gravel surfaces are sometimes confused with roads.

In general, when two surfaces have a similar material composition, some confusion errors can arise. Additional work has been performed to add information to the algorithms in order to discriminate between these different types of cover, such as image fusion with multispectral Sentinel 2 scenes. This will allow more accurate differentiation between terrain features, roads and buildings. Information collected in the field observations also means that there is prior knowledge of some areas of the image, termed seed pixels, which are necessary to implement more accurate classification processes in future, through supervised methods. These tested and accurate supervised classifications will then be implemented in the rest of the optical image, allowing the findings to be extrapolated to other regions affected by the same earthquake, while also optimizing the processes through integration with Geographic Information Systems. The same principle works if we use SAR instead of applying optical images, for example, through SAR differential polarimetry [29,30].

5. Data Collection in the Field

The field campaign was conducted in November 2023, two months after the earthquake, visiting the areas identified through geospatial images and pre-processing. Surveys were carried out to assess the condition of the buildings post-event and images were captured for subsequent analysis in the office. During the inspections, the absence of debris collection work in the aftermath of the earthquake was noted. Most of the debris was still on the streets in which it fell, as can be seen in the photographs provided in this section.

5.1. Post-Processing of Geospatial Images Following Field Campaign

The relationship between the spatial patterns of earthquake damage and intensity was studied by contrasting the observations made during the visit with the data from the previous geospatial analysis, leading to some interesting findings. Firstly, Tafeghaghte and Talat N'Yaaqoud, two of the sites most devastated by the earthquake, are practically the same distance from the epicenter and symmetrical to it in terms of east–west orientation. However, the predominant construction systems in each of the analyzed locations were markedly different from a seismic vulnerability perspective. According to the EMS98 manual [31], constructions can be arranged into six classes in terms of vulnerability, from A (most) to F (least vulnerable), and the damage they sustain can fall into five grades, from 1 (negligible to slight damage) to 5 (destruction). Furthermore, the earthquake intensity at each location, from degree I (not felt) to XII (completely devastating) can be characterized according to a scale that takes into account the effects on humans, objects and nature, as well as the grade of damage to buildings with respect to their vulnerability class. The latter parameter is that which can be most objectively evaluated by seismic engineering experts in a field campaign.

In accordance with the EMS manual [31], the structures in Tafeghaghte, primarily composed of stone masonry with non-anchored one-way wooden floorings, are categorized as Class A vulnerability. Most of these buildings had collapsed (grade 5), whereas confined masonry constructions suffered less damage (grade 2 to 4), suggesting an intensity of approximately IX in this area (Figure 7). In contrast, in the analyzed area of Talat N'Yaaqoub there were numerous constructions with confined masonry walls made of concrete blocks with beam and block floorings, classified as Class C vulnerability [31]. A less-vulnerable construction system recommended by Moroccan seismic regulations and other guidelines

in regions with high seismic-threat [13,32] suffered damage ranging from Grade 3 to 5 in many buildings. The macroseismic intensity in this zone is estimated to fall within Grade X, according to the damage observed to the constructions (Figure 8).

Figure 7. Evaluation of damage along a street in Tafeghaghte subsequent to the 8 September 2023 earthquake. Stone masonry structures have predominantly collapsed, while confined masonry systems or confined mixed systems mostly display damage ranging from grade 2 to 4 [31].

Figure 8. Assessment of damage in a street of Talat N'Yaaqoub following the 8 September 2023 earthquake. Confined masonry structures exhibit extensive destruction, with buildings suffering grade 3 or higher damage, and numerous collapses recorded at grade 5 [31].

Differential Interferometric Synthetic Radar (DInSAR) Approach

The integration of these results with SAR data has made it possible to establish relationships between ground deformations, geometric trajectories, and possible topographic effects, which must be analyzed in future research. A Sentinel 1 interferometric pair was processed from images taken on the 3 and 15 September 2023 (Figure 5b). The results from the advanced SAR processing can be updated continuously and, thus, integrated into the Geographic Information Systems along with the rest of the information generated, with the

aim of exploring the possibilities provided through their interconnection, throughout the region, with other places not visited in November but also affected by the earthquake of 8 September 2023.

Taking into account that Sentinel 1 operates in Band C in a frequency range between 4 and 8 GHz and wavelengths between 7.5 and 3.75 cm, and by virtue of the phase scale, counting the fringes where the band colors begin to look consistent between the epicenter and near the visited areas, the DInSAR interferogram (Figure 9) allows estimating that the ground around the epicenter moved downwards (away from the satellite) from 8 cm to 30 cm in the places analyzed sometime between the interferometric-pair dates 3 and 15 September 2023. The earthquake was on 8 September, which suggests that this was inflation associated with the earthquake.

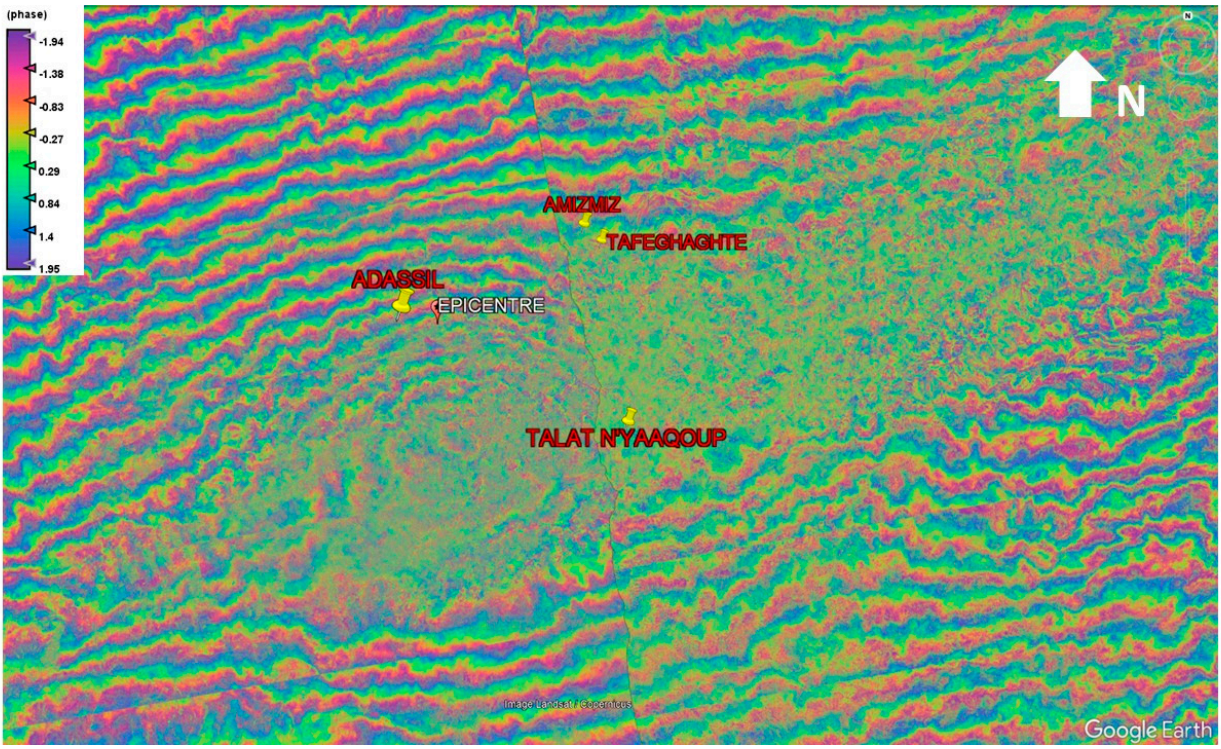

Figure 9. Detail of the differential interferogram DInSAR computed from Sentinel 1 radar images (3–15 September 2023) for Amizmiz, Adassil, Tafeghaghte and Talat N'Yaaqoud. Surface displacements upwards (towards the satellite) or downwards (away from satellite) in the line-of-sight direction of the satellite.

According to the estimations over the computed DInSAR interferogram, in the visited areas the surface moved upwards in Adassil by an amount ranging from 8 to 12 cm, in Tafeghaghte by 19 to 23 cm, in Amizmiz by 19 to 23 cm and in Talat N'Yaaqoud by 23 to 27 cm. Furthermore, an apparent topographic effect, that is, surface uplifts and surface subsidence, was observed in the cases of Tafeghaghte and especially Talat N'Yaaqoud.

5.2. Construction Characteristics and Observed Damage in Identified Building Systems

As regards seismic vulnerability, the general characteristics of buildings observed in the field campaign highlighted poor material quality, insufficient seismic-resistant design, and the use of unskilled labor in both traditional and modern constructions. Poor construction is usually due to a lack of knowledge regarding the inadequacy of certain practices for seismic-prone areas, especially in terms of the connection of structural elements and the quality of construction materials, which can be difficult to verify during visual inspection [33]. In the in situ construction assessments, standardized forms are usually

employed. In this study, following a review of the survey forms adopted in other countries around the world, the form currently used in Italy (the AeDES form) was chosen [27,34], focusing particularly on the elements which highlight the role of vulnerability in the final usability evaluation.

Table 3 summarizes the typologies found in the different areas and the main attributes associated with each. A more detailed description is provided below.

Table 3. Summary of typologies found in the areas visited in the High Atlas. A mixed typology was observed, where the first floor(s) was constructed with rammed-earth walls or unreinforced stone masonry walls, while the upper floors were constructed with masonry-filled reinforced concrete (RC).

Structural Lateral System (Typical Thickness)	Flooring System	Typical Number of Floors	Schema
Traditional Construction			
Rammed-earth wall (50 to 60 cm)	Wooden beams covered with straw and compacted earth	1 to 3	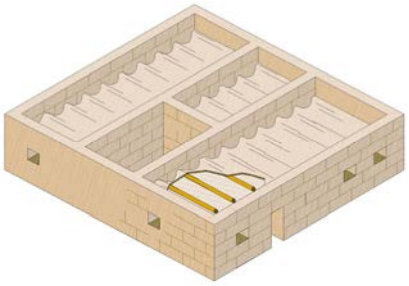
Unreinforced stone masonry walls: rounded or quarry stones bound together with a weak, irregularly bonded mud mortar (40 to 90 cm)	Unidirectional wooden flooring system filled with straw and a layer of mortar or rammed earth	1 to 2	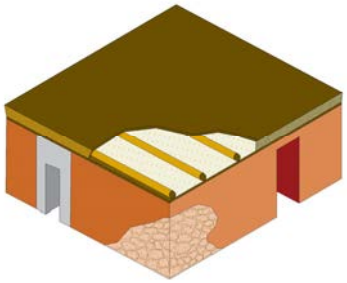
Modern Construction			
Mixed: hybrid behavior between masonry-filled RC frame structures working in flexure and confined (with RC beam and columns) shear-resistant masonry wall structures (10 to 25 cm)	RC joists and concrete hollow blocks with a reinforced or unreinforced compression deck layer	1 to 4	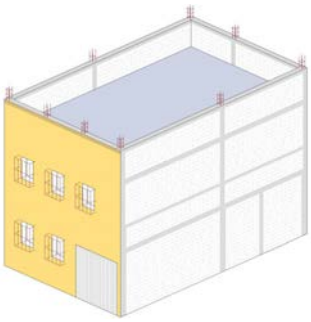

5.2.1. Traditional Construction

The traditional construction methods prevalent in the rural mountainous regions of Morocco involved the use of structures built using rammed earth, mud bricks, and stone. These construction techniques often exhibit brittle behavior owing to the inferior quality of materials and the bonding characteristics, thereby posing a risk of sudden or partial collapse. Furthermore, the substandard quality of mortar, prone to easy cracking, contributes significantly to reduced stiffness and may underlie local and widespread structural failures. In the areas visited, the buildings identified were mostly of rammed

earth and unreinforced stone masonry construction. The characteristics analyzed and the most common damage observed are presented below.

- Rammed-earth wall

Single and two- or three-story residential houses comprise load-bearing earth walls ranging in thickness from 50 to 60 cm. Over time, the material tends to lose cohesion. The floor slabs are typically heavy, consisting of wooden beams covered with straw and compacted earth. There is often a lack of diaphragms, inadequate support, and an absence of anchoring of floor and roof elements to walls, leading to highly flexible floor systems and deficient roof structures (Figure 10). Moreover, due to the lack of cohesion, characteristic of this material, perpendicular walls present a lack of box behavior. The vulnerability of this type of construction is not included within the classification provided by the EMS-98; however, its main features make these buildings more vulnerable than those considered the most vulnerable in this scale, those in Class A. Therefore, it would be reasonable to consider them as not classified (equal or inferior to class A).

(**a**) (**b**)

Figure 10. Out-of-plane failure of an exterior wall on a rammed-earth building with a floor constructed from wood, straw, and mud. These images highlight insufficient connectivity observed between the perpendicular walls and the floor diaphragms. Image (**a**) displays damage to the corner and a portion of the parapet and image (**b**) illustrates an out-of-plane failure of a wall. The buildings were situated in the central area of Adassil.

- Unreinforced stone masonry walls

In the study area, this system comprises load-bearing walls constructed with rounded or quarry stones bound together with a weak, irregularly bonded mud mortar. The thickness varies from 40 to 90 cm. These walls comprise stones arranged to form both an inner and outer face, with filling material in between. As this filling material tends to be weaker due to deterioration over time, this potentially gives rise to two independent walls. Most of the buildings observed had a unidirectional wooden flooring system. Intermediate floors typically consist of a load-bearing wooden structure filled with straw and a layer of mortar or rammed earth. These structures are heavy and offer limited resistance to lateral loads due to the lack of connection between vertical and horizontal elements (Figure 11). In preliminary research carried out in Italy, the most vulnerable structures identified consisted of masonry buildings with an irregular plan (uncoated stone), flexible floors and

a lack of adequate connections, very similar to the structures found in the study area [17]. The practical construction design guide [32], published in conjunction with the national standard, emphasizes that effective construction practices for this type of masonry involve establishing a robust connection at the roof level. Additionally, it advises against the use of round stones, which are prevalent in the study area, and highlights the importance of meticulously addressing corner stones.

(**a**) (**b**)

Figure 11. Impact of the 8 September 2023 earthquake on a stone masonry building with wooden log slab in Amizmiz. Image (**a**) illustrates the inward collapse of the roof, attributed to inadequate support, leading to the subsequent collapse of the upper part of the wall. Image (**b**) shows the crumbling of the walls.

Structural Damage in Traditional Construction Systems

Traditional structures presented differing behavior depending on the location and topography of the site. In Tafeghaghte, 23 km from the epicenter, the destruction of traditional houses, mostly made of stone masonry, was very severe. In contrast, in Adassil, 5 km from the epicenter, the level of destruction was lower (Figures 10 and 12), with a minor incidence of dwellings with high grade of damage [31] located on a hillside and in the center of the village, where the structures were mostly of rammed earth.

Figure 12. Impact of the 8 September 2023 earthquake on a traditional building in Adassil with a floor made of wood, straw, and mud. The observed damage includes the disintegration of sections of the stone masonry walls of the house and failure characterized by perpendicular bending at the corners of the rammed-earth dwelling.

The most prevalent failure mode identified in traditional structures was the partial or complete overturning of walls out-of-plane, as depicted in Figure 12. This failure pattern is commonly associated with inadequate connections between perpendicular walls or floors [35,36]. In stone masonry, such failure is frequently witnessed in instances of wall collapse caused by weak mud mortar, inadequately integrated multi-leaf stone wall construction, and insufficiently supported floors [37].

In the context of isolated or corner buildings, particularly those constructed with rammed earth, corner failure was also observed. This type of failure was more prone to occur in scenarios where nearby openings (Figure 13) or structural designs contributed to an accumulation of stress at the corners. In the case of construction systems using earth, observed specifically in the study of Adassil, the rammed-earth buildings with a quadrangular shape and a central patio exacerbated the concentration of stress at re-entrant corners, as illustrated in Figures 10 and 12. This behavior was also observed in stone masonry, where the concentration of stress in tension and the irregular shape of the building was the cause of the observed damage (Figure 14).

(**a**) (**b**)

Figure 13. Damage assessment of a traditional rammed-earth building depicting various stages of damage. The corner failure is exacerbated by the presence of window openings. (**a**) Partial corner failure, (**b**) Total corner failure.

Figure 14. Damage observed in an L-shaped masonry residential structure. The damage at the corner is evident, attributed to concentration of stress in this specific area. Residential dwelling in the vicinity of Tafeghaghate.

In Amizmiz and Talat N'Yaaqoub, this traditional type of construction was also present, in either the whole dwelling (Figure 11) or only the lower floors. In the latter case, this

situation arose because the dwellings had grown vertically over time, adding more stories according to the residents' needs but using different construction systems (Figure 15). The brittleness and limited ductility of the stories built using traditional materials determined the behavior of the whole building. The difference in rigidity between the construction elements was decisive in the seismic response of the buildings. Furthermore, the difficulty involved in adequately connecting the two construction systems underlies the fact that many buildings presented damage resulting from sliding between lower walls and upper floors of differing materials (Figure 15b). Additionally, the positioning of these dwellings within the aggregate might influence their seismic response [38–40].

(**a**) (**b**)

Figure 15. Traditional ground-floor buildings with upper floors constructed using reinforced masonry. Image (**a**) shows evident inadequate connections between traditional and modern construction elements. Image (**b**) illustrates the lack of connection, combined with varying stiffness among the floors, resulting in the manifestation of horizontal cracks. Location: Amizmiz and Tafeghaghate.

5.2.2. Modern Construction

In the study regions of Morocco, modern construction methods [33] were prevalent in the population centers and locations connected with economic activity and, to a minor degree, in the rural areas. These constructions involve the use of masonry and reinforced concrete (RC) structural systems. The characteristics of the constructions and deficiencies observed in terms of vulnerability of these buildings are described in this section, highlighting poor material quality, insufficient seismic-resistant design, and the use of unskilled labor.

In the areas visited, the most recent buildings of non-traditional construction style were found to be primarily constructed using a combination of RC and masonry as materials. This complexity of the structural arrangement made it difficult to accurately classify the lateral load-resistant systems. Essentially, they presented a hybrid behavior between masonry-filled RC frame structures working in flexure and confined (with RC beam and columns) shear-resistant masonry wall structures, defined as a mixed system under the current Moroccan regulation, the RPS 2000 version 2011. Hence, the mixed system is defined as being composed of frames and walls, the resistance of which to seismic forces is ensured by both the walls and frames, proportionally to their respective stiffness (RPS2000 version 2011, 1.2.3. mixed system [13]).

According to the observations, most of these confined masonry and RC constructions have certain characteristics in common. Generally, they have up to four stories, except for those of special interest to the population such as mosques. These stories may be constructed at the same time or in successive phases, using masonry infill materials with

similar or different characteristics. In this regard, it is common to find starter bars at the top of columns to facilitate the anchorage of RC elements of future upper stories (see Figure 16).

Figure 16. Several buildings with starter bars at the top of columns to facilitate the anchorage of RC elements of future upper stories (Amizmiz).

Furthermore, with regard to structure, the horizontal elements were mainly composed of RC joists and concrete hollow blocks with a reinforced or unreinforced compression deck layer (Figure 17a,b). In these cases, a diaphragmatic effect of floor systems is unlikely, due to the low quality of the components and the weak connection between horizontal and vertical elements. Nonetheless, exceptionally, a few cases were identified of reinforced concrete slabs with extremely high ductility in comparison with the vertical structures (Figure 17c).

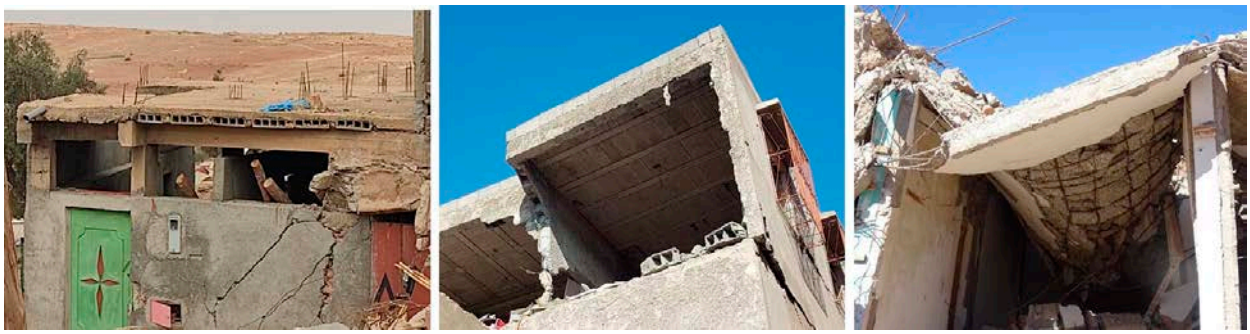

(**a**) (**b**) (**c**)

Figure 17. Several buildings with starter bars at the top of columns to facilitate the anchorage of RC elements of future upper stories. (**a**) Tafeghaghte, (**b**) Amizmiz, (**c**) Talat N'Yaqoud.

Concerning the construction practices employed in buildings pertaining to the mixed systems identified, the following findings were obtained during the field campaign. The team observed that practically all those buildings presenting either severe damage or that had collapsed had not adhered to the good-practices recommendations with regard to the minimum strength and/or dimensions of RC sections or the area of longitudinal and transversal reinforcement described in well-known building codes (EC8 [41] and ACI-318 [42]). Furthermore, it should be noted that a number of these highly recommendable prescriptions from a seismic engineering perspective are not established in the applicable code, RPS 2000 version 2011. Moreover, a large number of buildings do not even comply

with the less restrictive measures included in the Moroccan code. These deficiencies resulted in structures showing insufficient stiffness, strength and/or ductility, as detailed below.

The compression strength of the concrete is one of the most important parameters for seismic behavior in both reinforced-concrete and confined masonry typologies. For this reason, some of the current building codes (EC8 and ACI-318) stipulate a minimum threshold of 20 MPa. In this regard, the RPS 2000 version 2011 establishes a minimum concrete compression strength of 22 MPa. Despite this legal requirement, the visual inspection of constructions revealed that the concrete quality was deficient in several aspects: visible porosity and cavities, discontinuous granulometry and the employment of large rounded aggregates (Figure 18). This low resistance and lack of cohesion of the material was also evidenced by its fragile rupture when exerting manual pressure. Furthermore, in some cases, the steel reinforcing bars were flat, unribbed, or with minimal ribs, which also contributed to poor overall behavior due to the extremely low adherence (see Figure 19). Only in a very small number of cases was corrosion of the steel reinforcement bars detected.

(**a**) (**b**) (**c**)

Figure 18. Low-quality reinforced concrete due to visible porosity and cavity/holes, discontinuous granulometry, and the employment of large rounded aggregates in structural elements pertaining to different buildings (Talat N'Yaqoud) (**a**–**c**).

(**a**) (**b**)

Figure 19. Deficiencies in steel bar reinforcement in concrete elements: (**a**) smooth bars; (**b**) presence of corrosion and minimal transversal ribs in longitudinal reinforcement (Talat N'Yaqoud).

Furthermore, the dimensions of the transversal sections of the columns and the steel stirrups were identified as being insufficient for both confined-masonry and RC frame constructions, given the damage observed, such as fragile failure (Figure 20). Additionally, the abovementioned dimensions were below those established in the RPS 2000 version 2011, which in turn are below those established in the EC8 and ACI-318 codes. Specifically, the steel stirrups were not only insufficient in number and sometimes inexistent, but also excessively distanced (Figure 20, details 1 and 2), in several cases exceeding 25 cm. In addition, widespread use of stirrups with hooks at 90° at their ends and reduced development length was detected, resulting in these elements opening more easily under the earthquake load. In this regard, reference regulations for RC with special requirements for seismic zones, such as ACI 318 [42], state that the hooks should have an angle of 135° and that the minimum length should be six times the diameter of the bar and longer than 75 mm (Figure 20, detail 1). Similarly, it was observed that overlapping of the longitudinal steel bar reinforcements was frequently carried out in areas of greatest demand, for example, near the beam–column joints. Moreover, it was found that the development length of the longitudinal steel reinforcement was insufficient at the junction of beams with end columns (Figure 20, detail 3).

(**a**) (**b**)

Figure 20. Deficiencies in RC elements that lead to low-ductility sections and fragile failure. Details 1 and 2: fragile failure in the support at the floor-support-system joint due to low-quality concrete, excessive distance between steel stirrups at a critical point, and non-earthquake-proof hooks (<135° or length less than 6φ or 75 mm) in the joint. Detail 3: short development length and deficient anchoring of steel for longitudinal reinforcement of the beam where it connects with the column. (**a**) Amizmiz; (**b**) Talat N'Yaqoud.

Additionally, the observed modern constructions exhibiting behavior similar to confined shear-resistant masonry wall structures deserve specific study, as they presented a number of particular features and damage.

- Confined shear-resistant masonry wall structures

Firstly, as regards the specific constitution of the shear-resistant masonry walls, the confining reinforced concrete components presented the deficiencies detailed above. The masonry components, however, were predominantly made from hollow cement–mortar pieces with low resistance to compression, easily identifiable in a visual inspection. As shown in Figure 21a, the components present very low cell thickness, around 1 cm, which considerably decreases their transversal section. Moreover, the cement–mortar joints between pieces are sometimes much thicker on their horizontal faces (Figure 21b), non-uniform, and highly variable in thickness. These factors, in part, account for the generalized poor performance of masonry buildings, which presented extreme damage and numerous complete collapses. Similarly, some of the mixed structures observed combined cement–mortar hollow-block masonry walls of very dissimilar characteristics or these elements combined with solid blocks of mortar or hollow pieces of fired clay or natural stone, or, in some cases, even a combination of various of these materials (Figure 21c). The effect of the combination of different confined materials on the structural behavior of the buildings has proven to be highly significant. Figure 22 shows the highly dissimilar results for the different materials combined in the same construction: the parts of the wall constructed of concrete blocks withstood the earthquake, whereas the stone parts collapsed.

(**a**) (**b**) (**c**)

Figure 21. (**a**) Cement–mortar blocks (Tafeghaghte). (**b**) Bed joints (Amizmiz). (**c**) Different types of masonry of highly dissimilar quality in the same wall (Tafeghaghte).

Figure 22. Comparison of damage for different infill materials in the same wall (Tafeghaghte).

Similarly, low-quality connections between vertical elements and low-quality materials were identified as factors causing out-of-plane failure of walls (Figure 23). Mention should be given to cases of some buildings combining RC frames and masonry walls presenting out-of-plane failure of infill walls. This occurred either due to inefficient connection (Figure 23c) or inadequate sequencing during the execution of the different components: reinforced concrete beams and columns were erected before the block walls, leading to poorer structural behavior than would be the case in a confined masonry structure with the same quantity of materials (Figure 23c). Moreover, some buildings presented confining beams and columns which were poorly bounded to extremely low-shear-strength hollow concrete blocks, which failed during the seismic event (Figure 23a).

(**a**) (**b**) (**c**)

Figure 23. Out-of-plane failures: (**a**) a confined masonry load-bearing wall and parapet wall because of the low-quality materials employed (Amizmiz). (**b**) Failure of a masonry wall with RC beams and columns due to the low shear strength of the masonry employed (Amizmiz). (**c**) Out-of-plane failure of a masonry wall with RC beams and columns due to inappropriate order of execution of components (Amizmiz). The structure does not behave as a confined masonry structure.

Additionally, the high number of collapsed parapets, despite having masonry confining columns, is particularly significant due to the low quality of the reinforced concrete and concrete blocks used (Figures 23a and 24).

Figure 24. Out-of-plane failure of confined masonry parapet walls in two buildings with different structural wall material (Tafeghaghte) (**both**).

Finally, a key aspect of these structures that should not be ignored is the scarcity of confining elements found. Most buildings presented a lack of RC elements that confined the masonry in the door and window openings (Figure 25). This absence facilitated the openings acting as weak point determinant for the damage in the resistant walls.

Figure 25. Damage mainly due to the absence of reinforced-concrete confining elements in door and window openings (Amizmiz) (**all**).

5.2.3. Structural Design and Modifiers Related to the Position of Dwellings in the Block

Along with the inadequate materials and construction techniques described, the buildings in the study area presented several structural design deficiencies and other factors related to their position with respect to other neighboring buildings [43], which affected their vulnerability. These aspects include types of damage widely described in the literature [44,45] and more singular and less documented kinds of damage, as they correspond to less-common structural systems found in the area. These factors affecting building vulnerability are described below.

- Structural design

Firstly, a crucial factor was the absence of a structural system providing resistance and stiffness in both orthogonal directions, capable of withstanding seismic effects in either direction. In the most critical cases, floor slabs are directly supported by walls, also designed in only one direction, with limited or no presence of orthogonal walls. Figure 26 shows two examples of buildings structured in a single direction.

(**a**) (**b**)

Figure 26. Buildings presenting a structural system which provides seismic resistance and stiffness mainly in only one of the two orthogonal directions. (**a**) Amizmiz; (**b**) Tafeghaghte.

Moreover, the irregularity in elevation constituted a determining factor in the collapse of numerous structures within the zone. This deficiency in the structural integrity may be caused by the presence of a 'soft' or flexible story (lower stiffness) or a weak floor (lower resistance), both of which are seismic-vulnerability factors resulting in structural fragility and subsequent collapse.

In the areas visited, the architectural and structural origins of these disparities in rigidity or strength among different stories were identified. In several cases, a weak ground story was the cause of the collapse of buildings, with the upper floors exhibiting substantially less damage (Figure 27a,b). In other cases, the damage was mainly concentrated in intermediate stories due to the presence of window openings (Figure 27c). It should be mentioned that this kind of damage is hardly identifiable through satellite images.

Two specific conditions resulting in irregularity in elevation are worth mentioning. The first of these was identified on slopes where significant differences in the lengths of vertical elements implied high vulnerability of the shortest elements (columns). Figure 28 illustrates cases in Talat N'Yaqoud, where, in addition to this deficiency, problems of instability of the slope and possible topographic amplifications were detected. The second condition, identified in several buildings, is associated with the employment of very different structural materials for the lateral load-bearing walls of each floor (Figure 21c).

Furthermore, there are marked geometrical dislocation from one floor to the next, as well as highly dissimilar total floor areas in the different stories of the building, which causes the stiffness and mass centers to be far from each other, leading to the appearance of torsional forces on the building. In the field campaign, these seismic-resistant design defects were not as commonly found as weak stories, since most buildings were small-to-medium-sized houses. However, some buildings presented a high number of irregularities in terms of elevation and/or plan (Figure 29).

(**a**) (**b**) (**c**)

Figure 27. (**a**) Building in which the minor presence of shear-resistance walls on the ground floor resulted in a weak ground-story overturning failure (Amizmiz). (**b**) Building in which the excessive number of doors on the ground floor, which is characteristic of commercial buildings in the same road, causes a weak ground-story overturning failure (Talat N'Yaaqoud). (**c**) Building with major damage mainly concentrated in the intermediate story, due to window openings (Amizmiz).

Figure 28. Buildings located on slopes and presenting very different column lengths (Talat N'Yaqoud).

(**a**) (**b**) (**c**)

Figure 29. (**a**,**b**): state of a building before and after the earthquake (red dots). The building exhibited a high number of irregularities in height and plan, such as differences in stiffness and strength and balconies. p1 and p2 are inserted as reference points (Talat N'Yaaqoud). (Source photo before the earthquake: Google Maps, https://www.google.es/maps/place/Talat+N%E2%80%99Yaaqoub,+Marruecos, accessed on 18 January 2024). (**c**) Building with a marked height irregularity between the ground floor and the rest, along with columns displaced from the same vertical line. Possible torsional effects due to the presence of a much more rigid, blank dividing wall and the three very open façades facing the street (Amizmiz).

- Urban position

Previous seismic events and research into these events have shown the importance of the position in the block [40,46–50] and the pounding effects [38,51] between adjacent

buildings on the seismic vulnerability. The seismic performance of masonry building aggregates is often affected by the presence of fragile and deformable floor membranes, along with asymmetrical geometries. These factors contribute to complex and challenging dynamic actions, leading to various in-plane and out-of-plane responses of each structural unit [52]. Also, the location of a building on a corner or at one end of a row of buildings has been shown to increase the probability of suffering greater damage during a seismic event. For example, the position on a corner, due to dissimilar walls in terms of stiffness, can result in torsion. Hence, the shear resistance of the walls and the presence of well-designed holes in the walls have proven to be crucial factors to withstand an earthquake. This factor has mainly been identified in combination with other modifiers such as pounding effects, which can be produced by more rigid, resistant elements adjacent to the building (Figure 30).

Figure 30. Building on a corner where a lower, more rigid adjacent construction has caused very noticeable pounding effects (Amizmiz).

Additionally, some other buildings presented damage which was highly influenced by a combination of several of the factors mentioned previously: an urban modifier in combination with a structural design deficiency and a number of construction deficiencies. Figure 31 shows a building in which the presence of a weak story, pounding effects from the adjacent building, and deficiencies in the concrete and reinforcement of beams and columns account for its collapse.

Figure 31. Building located on a corner, collapsed and overturned, presenting a possible weak-story deficiency and pounding effects from the adjacent building. Detail 1. Low resistance of the concrete and areas of low-longitudinal-reinforcement steel in the beam and the column. Short length of development and anchoring of steel for longitudinal reinforcement of the beam where it connects with the column. Absence in the beam of the recommended first closed confinement stirrup located no more than 50 mm from the face of the support element (ACI-318). Excessive distance between transversal reinforcement in a critical point of the column and absence of seismic hooks at the ends of the column stirrups (Amizmiz).

6. Conclusions and Future Lines of Research

The seismic event that occurred in September 2023, with a magnitude of Mw = 6.8, was one of the most powerful earthquakes to impact the Atlas region of Morocco. Fatalities within the study area predominantly resulted from either complete or partial collapse of structures. This paper provides an overview of the seismological aspects of the earthquake and briefly outlines the damage sustained in four selected villages, employing a prior study of the region through satellite images and an in situ study of constructions.

As regards the analysis through satellite images, modeling of the multispectral data and SAR can yield information on the depth and dynamics of the seismological system. In this research, the usefulness of approximate geospatial analysis for the planning of the campaign itself was confirmed, and for geospatial monitoring in future research, using techniques that minimize the errors that prior approximation necessarily contains. Future research should employ a multitemporal and multisource research strategy to achieve a more in-depth analysis.

The results from the field campaign highlight the fact that poor material quality, inadequate earthquake-resistant design and the use of unskilled labor were the main causes of the damage in both traditional buildings and more recent building designs in the area. Although traditional constructions exhibited a greater degree of damage, confined block masonry construction in the Talat N'Yaaqoud area also showed a significant degree of damage. Additional effects are considered to have amplified the seismic wave and the subsequent damage, beyond the quality of the construction and its design.

The damage observed evidences the fact that unconfined and unreinforced masonry should not be employed in new building construction in high-hazard seismic areas. Similarly, the use of reinforced-concrete confined masonry structures should be limited to regular, low-rise structures and safety factors should be reviewed for the design, since the variability in quality of materials and workmanship will highly influence the likelihood of brittle failure. Furthermore, existing structures made of these materials must be reinforced, paying special attention to the interlocking between walls and connections between walls and floors/roofs.

Future research endeavors should focus on investigating whether the terrain, slope, and topography played a substantial role in influencing the structural behavior of buildings in the Talat N'Yaaqoud area, which were constructed using a confined masonry typology with concrete blocks. Although it is clear that the abovementioned construction and design shortcomings have increased vulnerability of buildings in this village, the results of this research seem to suggest that other factors may also have contributed to the fact that this region suffered a greater level of damage compared to areas situated at similar or even closer distances to the epicenter. Investigating and quantifying the potential amplification of seismic waves due to geographical factors, and their interaction with structural vulnerabilities, could yield valuable insights to enhance seismic resilience in comparable environments.

Author Contributions: Conceptualization, B.G.-R., L.N.-S., J.G.R.-A., O.H.-R. and M.B.B.; Methodology, B.G.-R., L.N.-S., J.G.R.-A., O.H.-R. and M.B.B.; Software, J.G.R.-A.; Validation, B.G.-R., L.N.-S., J.G.R.-A. and M.B.B. Formal analysis, B.G.-R., L.N.-S., J.G.R.-A., O.H.-R. and M.B.B.; Investigation, B.G.-R., L.N.-S., J.G.R.-A., O.H.-R. and M.B.B.; Resources, B.G.-R. and M.B.B.; Data curation, B.G.-R., L.N.-S., J.G.R.-A., O.H.-R. and M.B.B.; Writing—original draft, B.G.-R., L.N.-S., J.G.R.-A., O.H.-R. and M.B.B.; Writing—review & editing, B.G.-R. and L.N.-S.; Visualization, B.G.-R., L.N.-S. and O.H.-R.; Supervision, B.G.-R. and M.B.B.; Project administration, B.G.-R.; Funding acquisition, B.G.-R. All authors have read and agreed to the published version of the manuscript.

Funding: This research received no external funding.

Data Availability Statement: Data is contained within the article.

Acknowledgments: The authors are grateful to the Cooperation Platform of Universidad Politécnica de Madrid and the seed project "Analysis of the improvement of the behavior of reinforced adobe walls in the face of seismic action" for supporting the research. The authors are also thankful to

Carlos Gamboa for his assistance with GIS management and seismicity figure editing and to image processing facilities funded by the Industrial Doctorate of Madrid Region Projects (IND2020/TIC-17528 IND2023/TIC-28743). We are very grateful to the population of the study area for providing information and logistical support.

Conflicts of Interest: Author Orlando Hernández-Rubio was employed by the company Geolyder SL. The remaining authors declare that the research was conducted in the absence of any commercial or financial relationships that could be construed as a potential conflict of interest.

References

1. Peláez, J.A.; Chourak, M.; Tadili, B.A.; Brahim, L.A.; Hamdache, M.; Casado, C.L.; Solares, J.M.M. A Catalog of Main Moroccan Earthquakes from 1045 to 2005. *Seismol. Res. Lett.* **2007**, *78*, 614–621. [CrossRef]
2. Alami, M.H.; Günay, S.; Mosalam, K.M.; Vargas, L.; Hassan, W.M.; Bektas, N.; Martin, A.; Nobahar, M.; Romão, X.; Zaoui, H.; et al. Morocco Earthquake Preliminary Virtual Reconnaissance Report (PVRR), Virtual. 2023. Available online: https://www.steer.network (accessed on 5 December 2023).
3. Cherkaoui, T.E.; El Hassani, A. Seismicity and Seismic Hazard in Morocco 1901–2010. *Bull. l'Institut Sci. Sect. Sci. Terre* **2012**, *34*, 45–55.
4. Jiménez-Munt, I.; Torne, M.; Fernández, M.; Vergés, J.; Kumar, A.; Carballo, A.; García-Castellanos, D. Deep Seated Density Anomalies Across the Iberia-Africa Plate Boundary and Its Topographic Response. *J. Geophys. Res. Solid Earth* **2019**, *124*, 13310–13332. [CrossRef]
5. El Moudnib, L.; Timoulali, Y.; Nouayti, A.; El Abbassi, M.; Bouka, M.; Nouayti, N.; Mhammdi, N. Seismotectonic model of High-Middle Atlas Junction (Morocco) derived from earthquake focal mechanism and stress tensor analysis. *Model. Earth Syst. Environ.* **2023**, *9*, 2407–2423. [CrossRef]
6. Sébrier, M.; Siame, L.; Zouine, E.M.; Winter, T.; Missenard, Y.; Leturmy, P. Active tectonics in the Moroccan High Atlas. *Comptes Rendus Geosci.* **2006**, *338*, 65–79. [CrossRef]
7. U.S. Geological Survey. M 6.8—Al Haouz, Morocco, Earthquake Hazards Program. 2023. Available online: https://earthquake.usgs.gov/earthquakes/eventpage/us7000kufc/executive (accessed on 18 January 2024).
8. Euro-Mediterranean Seismological Centre. Quick Moment Tensors Solutions, EMSC. Available online: https://emsc-csem.org/Earthquake_data/data.php?type=mt&id=1550978&base=GCMT_ICYMNKFTD&sub=TD&auth=GCMT&Y=2023&M=09&D=08 (accessed on 18 January 2024).
9. Euro-Mediterranean Seismological Centre. Felt Report, EMSC. 2023. Available online: https://emsc-csem.org/Earthquake_information/earthquake_map.php?id=1550978 (accessed on 18 January 2024).
10. Rodríguez-Navarro, P.; Vidal, F.J.; Gil-Piqueras, T.; Fantini, F. Earth construction techniques in the Nortern High Atlas, Morocco. In *Rammed Earth Conservation*; Mileto, C., Vegas, F., Cristini, V., Eds.; Taylor & Francis, Ed.: Oxfordshire, UK, 2012; pp. 569–574.
11. Costa, M.R.; Batista, D. Architecture traditionnelle dans les zones de montagne: Contribution à l'étude de la typologie des habitations dans le Haut Atlas au Maroc. *Digit.-Rev. Digit. de Arqueol. e Arquit. Artes* **2018**, *2018*, 373–397. [CrossRef]
12. *RPS 2000, Règlement de Construction Parasismique*; Ministère de l'Habitat et de la Politique de la Ville LE: Rabat, Morocco, 2002.
13. RPS 2000 Version 2011. Règlement de Construction Parasismique. 2011. Available online: https://www.sodibet.com/telechargement/RPS2011.pdf (accessed on 1 March 2024).
14. Preciado, A.; Santos, J.C. Rammed earth sustainability and durability in seismic areas as a building material. *IOP Conf. Ser. Earth Environ. Sci.* **2020**, *410*, 012108. [CrossRef]
15. Adhikari, R.K.; D'Ayala, D. 2015 Nepal earthquake: Seismic performance and post-earthquake reconstruction of stone in mud mortar masonry buildings. *Bull. Earthq. Eng.* **2020**, *18*, 3863–3896. [CrossRef]
16. Briseghella, B.; Demartino, C.; Fiore, A.; Nuti, C.; Sulpizio, C.; Vanzi, I.; Lavorato, D.; Fiorentino, G. Preliminary data and field observations of the 21st August 2017 Ischia earthquake. *Bull. Earthq. Eng.* **2019**, *17*, 1221–1256. [CrossRef]
17. Penna, A. Seismic assessment of existing and strengthened stone-masonry buildings: Critical issues and possible strategies. *Bull. Earthq. Eng.* **2015**, *13*, 1051–1071. [CrossRef]
18. Chidiac, S.E.; Foo, S. *Guidelines for the Seismic Upgrading of Stone-Masonry Structures*; Public Works & Government Services Canada: North York, ON, Canada, 2002; Volume 84. [CrossRef]
19. Dizhur, D.; Dhakal, R.P.; Bothara, J.; Ingham, J.M. Building typologies and failure modes observed in the 2015 Gorkha (Nepal) earthquake. *Bull. N. Zealand Soc. Earthq. Eng.* **2016**, *49*, 211–232. [CrossRef]
20. Murphy, P. *Al-Hoceima Earthquake 24 02 2004*; Seismic Engineering: Madrid, Spain, 2004.
21. Bothara, J.K.; Hiçyılmaz KM, O. General observations of building behaviour during the 8th October 2005 Paquistan earthquake. *Bull. N. Zeal. Soc. Earthq. Eng.* **2008**, *41*, 209–233.
22. Rejas Ayuga, J.G.; Martínez Marín, R.; Malpica Velasco, J.A. Hyperspectral remote sensing application for semi-urban areas monitoring. In Proceedings of the 2007 Urban Remote Sensing Joint Event, Paris, France, 11–13 April 2007. [CrossRef]
23. Masi, A.; Chiauzzi, L.; Santarsiero, G.; Liuzzi, M.; Tramutoli, V. Seismic damage recognition based on field survey and remote sensing: General remarks and examples from the 2016 Central Italy earthquake. *Nat. Hazards* **2017**, *86*, 193–195. [CrossRef]

24. Pouget, M.; Madeira, J.; Le Floc'h, E.; Kamal, S. Caracteristiques spectrales des surfaces sableuses de la region cotiere nord-ouest de l'egypte: Application aux donnees satellitaires spot. *Caracter. Et Suivi Des Milieux Terr. En Reg. Arid. Et Trop.* **1991**, 27–38.
25. Huete, A.R. A soil-adjuste d vegetation index (SAVI). *Remote Sens. Environ.* **1988**, *25*, 295–309. [CrossRef]
26. Saito, R.; Spence, K. Rapid damage mapping using post-earthquake satellite images in IGARSS 2004. In Proceedings of the 2004 IEEE International Geoscience and Remote Sensing Symposium, Anchorage, AK, USA, 20–24 September 2004; pp. 2272–2275. [CrossRef]
27. Masi, A.; Santarsiero, G.; Digrisolo, A.; Chiauzzi, L.; Manfredi, V. Procedures and experiences in the post-earthquake usability evaluation of ordinary buildings. *Boll. Geofis. Teor. Appl.* **2016**, *57*, 199–200. [CrossRef]
28. Arthur, D.; Vassilvitskii, S. K-means++: The advantages of careful seeding. *Proc. Annu. ACM-SIAM Symp. Discret. Algorithms* **2007**, *7*, 1027–1035.
29. An, L.; Zhang, J.; Gong, L.; Li, Q. Integration of SAR image and vulnerability data for building damage degree estimation. In Proceedings of the 2016 IEEE International Geoscience and Remote Sensing Symposium (IGARSS), Beijing, China, 10–15 July 2016; pp. 4263–4266. [CrossRef]
30. Zhai, W.; Shen, H.-F.; Huang, C.-L.; Pei, W.-S. Building damage information investigation after earthquake using single post-event PolSAR image. In Proceedings of the 2016 IEEE International Geoscience and Remote Sensing Symposium (IGARSS), Beijing, China, 10–15 July 2016; pp. 7338–7341. [CrossRef]
31. Grünthal, G. *European Macroseismic Scale*; Council of Europe: Luxembourg, 1998; Volume 15.
32. Ministère de l'Habitat et de la Politique de la Ville. *Guide Practique D'utilitation du Reglement de Costruction Parasismique (RPS 2000 Version 2011)*; Ministère de l'Habitat et de la Politique de la Ville: Rabat, Morocco, 2013; pp. 1–201. Available online: https://www.mhpv.gov.ma/wp-content/uploads/2023/10/Guide-RPS-2011-V2011-Francais.pdf (accessed on 1 March 2024).
33. Cherif, S.-E.; Chourak, M.; Abed, M.; Douiri, A. Potential seismic damage assessment of residential buildings in Imzouren City (Northern Morocco). *Buildings* **2018**, *8*, 179. [CrossRef]
34. Taucer, F.; Pinto Vieira, A. Field Manual for Post-Earthquake Damage and Safety Assessment and Short Term Countermeasures (AeDES). *Eur. Comm.—Jt. Res. Cent.—Inst. Prot. Secur. Citiz. EUR 22868* **2007**, JRC37914.
35. D'Ayala, D.; Speranza, E. An Integrated Procedure for the Assessment. In Proceedings of the 12th European Conference Earthquake Engineering, London, UK, 9–13 September 2002.
36. D'Ayala, D.; Speranza, E. Definition of collapse mechanisms and seismic vulnerability of historic masonry buildings. *Earthq. Spectra* **2003**, *19*, 479–509. [CrossRef]
37. Bilgin, H.; Leti, M.; Shehu, R.; Özmen, H.B.; Deringol, A.H.; Ormeni, R. Reflections from the 2019 Durrës Earthquakes: An Earthquake Engineering Evaluation for Masonry Typologies. *Buildings* **2023**, *13*, 2227. [CrossRef]
38. Angiolilli, M.; Brunelli, A.; Cattari, S. *Fragility Curves of Masonry Buildings in Aggregate Accounting for Local Mechanisms and Site Effects*; Springer: Dordrecht, The Netherlands, 2023; Volume 21.
39. D'Ayala, D.F.; Paganoni, S. Assessment and analysis of damage in L'Aquila historic city centre after 6th April 2009. *Bull. Earthq. Eng.* **2011**, *9*, 81–104. [CrossRef]
40. Torres-Olivares, S.; González-Rodrigo, B.; Saavedra-Flores, E.I.; Feijoo-Mosquera, J.C. Seismic behaviour of reinforced—Masonry aggregate under different types of interaction between adjacent dwellings. *Bull. Earthq. Eng.* **2024**, *22*, 583–609. [CrossRef]
41. *UNE EN 1998*; EN1998 Eurocode 8: Design of Structures for Earthquake Resistance—Part 1: General Rules, Seismic Actions and Rules for Buildings. European Committee for Standardizatio: Brussels, Belgium, 2011.
42. *ACI 318R-05*; Building Code Requirements for Structural Concrete (ACI 318-05) and Commentary. ACI Committee: Farmington Hills, MI, USA, 2005.
43. Milutinovic, Z.V.; Trendafiloski, G.S. *RISK-UE An Advanced Approach to Earthquake Risk Scenarios with Applications to Different European Towns*; WP4: Vulnerability of Current Buildings; European Commission: Brussels, Belgium, 2003; pp. 1–111.
44. Lindeburg, M.R. *Seismic Design of Building Structures: A Professional's Introduction to Earthquake Forces and Design Details*; Belmont, C., Ed.; EEUU: Stanford, CA, USA, 1996.
45. Enrique, B.; Meli, R. *Diseño Sísmico de Edificios*; Limusa: Mexico City, Mexico, 2010.
46. Angiolilli, M.; Lagomarsino, S.; Cattari, S.; Degli Abbati, S. Seismic fragility assessment of existing masonry buildings in aggregate. *Eng. Struct.* **2021**, *247*, 113218. [CrossRef]
47. Battaglia, L.; Ferreira, T.M.; Lourenço, P.B. Seismic fragility assessment of masonry building aggregates: A case study in the old city Centre of Seixal, Portugal. *Earthq. Eng. Struct. Dyn.* **2020**, *50*, 1358–1377. [CrossRef]
48. Valente, M.; Milani, G.; Grande, E.; Formisano, A. Historical masonry building aggregates: Advanced numerical insight for an effective seismic assessment on two row housing compounds. *Eng. Struct.* **2019**, *190*, 360–379. [CrossRef]
49. Chieffo, N.; Formisano, A. Comparative Seismic Assessment Methods for Masonry Building Aggregates: A Case Study. *Front. Built Environ.* **2019**, *5*, 123. [CrossRef]
50. Formisano, A.; Ademovic, N. An overview on seismic analysis of masonry building aggregates. *Front. Built Environ.* **2022**, *8*, 966281. [CrossRef]

51. Miari, M.; Choong, K.K.; Jankowski, R. Seismic pounding between adjacent buildings: Identification of parameters, soil interaction issues and mitigation measures. *Soil Dyn. Earthq. Eng.* **2019**, *121*, 135–150. [CrossRef]
52. Chieffo, N.; Formisano, A.; Lourenço, P.B. Seismic vulnerability procedures for historical masonry structural aggregates: Analysis of the historical centre of Castelpoto (South Italy). *Structures* **2023**, *48*, 852–866. [CrossRef]